International Journal of Bridge Engineering (IJBE), Vol. 7, No. 3, (2019), pp. 49-72

SUSPENDED ARCH BRIDGES UNDER MOVING LOADS

A mathematical model for the 2D and 3D problem

Theodore G. Konstantakopoulos[1] and George T. Michaltsos[2]

[1]Civil Engineer PhD N.T.U.A., Greece
[2]National Technical University of Athens, Greece
e-mail: theokons@teemail.gr, michalts@central.ntua.gr

ABSTRACT: The present work studies the behavior of a suspended arch bridge under the action of concentrated or distributed moving loads, proposing a mathematical model for the problem. The studied suspended arch bridge has a dense arrangement of cables, while the described method can easily be extended in the case of a sparse arrangement of cables.

Two models are considered for the study of the bridge, a 2D model and a 3D one, while the theoretical formulation, is based on a continuum approach, that has been used in the literature to analyze such bridges. Finally the obtained equations are solved using the Duhamel's integrals and the Laplace Transform.

KEYWORDS: bridge dynamics; moving mass-loads; bouncing; irregularities.

1 INTRODUCTION

Arches provide a structural system that can efficiently support large loads while lending themselves to excellent aesthetics. Historically, arches have been widely used in bridge systems, however, in modern applications they are usually reserved for signature bridges, where aesthetics play an important role in the design. Because arches primarily resist loads through compression, steel and also concrete are ideal structural materials for their application.
In the last decades, the design practice for various types of steel structures, have been changed to limit state design rules to obtain more rational designs.

As for the steel arch structures, the classical critical instability is often regarded as the chief design criterion [1]. However, this is by no means the ultimate load, which the arches with practical proportioning can carry.

The papers studying the actual carrying capacity of arches with practical proportioning under practical loadings (i.e. circulation loads, earthquake's loads, support's motion etc), are considerably less than the ones studying the classical bifurcation buckling.

Among the studies relating to stability one should mention the Johnston's study [1] and also those of Bergermeister et al [2], Pircher et al [3], Wang et al

[4], Zhu and Sun [5], Bruno et al [6], Mannini et al [7] etc.

Among the studies relating to the creep phenomenon there is a lot of papers [8 to 15] relating, mainly, to the creep of concrete-filled steel arch tubes.

The actual carrying capacity of arches with practical proportioning under practical earthquake loadings is considerably less than those relating to the classical bifurcation buckling [16 to 20].

Finally there is a lack of papers relating to the supports' settlement and moving loads.

As for the supports' settlement, Drosopoulos et al [22] studied the behavior of stone arch bridge subjected to the abutment movement while Liu et al [22] studied the effect of a springing displacement.

As for the moving loads, there are papers related to masonry arch bridges [23] or hanger arch bridges [24-25] while the papers relating to the classical form of an arch bridge use numerical methods [26] or F.E. ones [27]. Few publications study the influence of moving trains as for example the paper of Calcada et al [28], Cher et al [29] or Wallin et al [30].

An arch bridge consists of three elements: the deck, the arch, and the cables (hangers) that connect deck and arch.

Although it is usual the dense arranged cables to be considered no deformable, in this study we consider them deformable in order to study their real behavior. In addition an initial lifting (negative deformation) of the deck has been considered, i.e. an initial tension of the cables in order to avoid the possible appearing compressive stresses.

Finally the form of the parabolic arch is given by the equation:

$$z(x) = \frac{4 \cdot f_o}{L^2} \cdot x^2 - \frac{4 \cdot f_o}{L} \cdot x \tag{1}$$

The present work studies the behavior of a suspended arch bridge under the action of concentrated or distributed moving loads, proposing a mathematical model for the problem. The studied suspended arch bridge has a dense arrangement of cables, while the described method can easily be extended in the case of a sparse arrangement of cables.

Two models are considered for the study of the bridge, a 2D model and a 3D one, while the theoretical formulation, is based on a continuum approach, that has been used in the literature to analyze such bridges. Finally the obtained equations are solved using the Duhamel's integrals and the Laplace Transform.

A variety of numerical examples allow one to draw important conclusions for structural design purposes.

1. INTRODUCTORY CONSEPTS

2.1. The arch

Let us consider the arch beam of figure 1, which the form is given by the

following equation:

$$z = z(x) \tag{2a}$$

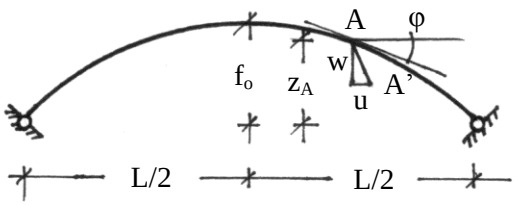

Figure 1. The arch

From the initial and the deformed state of an infinitesimal part ds of the arch we find:

$$\left.\begin{aligned} dx + du &= (1+\varepsilon)\cdot ds\cdot\cos(\varphi+\psi) \cong dx + \varepsilon\cdot dx - \psi\cdot dz \\ dz + dw &= (1+\varepsilon)\cdot ds\cdot\sin(\varphi+\psi) \cong dz + \varepsilon\cdot dz + \psi\cdot dx \end{aligned}\right\}$$

Or finally:

$$\left.\begin{aligned} du &= \varepsilon\cdot dx - \psi\cdot dz \\ dw &= \psi\cdot dx + \varepsilon\cdot dz \end{aligned}\right\} \tag{2b}$$

where, infinitesimal of higher order **$(\varepsilon\cdot dz\cdot\psi,\ \ \varepsilon\cdot dz\cdot dx)$** are neglected.

For a non-extensible beam (ε=0) we have:

$$\left.\begin{aligned} \frac{d\psi}{ds} &= \frac{d^2w}{dx^2}\cdot\frac{dx}{ds} \\ \frac{du}{dx} &= \varepsilon\cdot\left[1+\left(\frac{dz}{dx}\right)^2\right] - \frac{dw}{dx}\cdot\frac{dz}{dx} \end{aligned}\right\} \tag{2c}$$

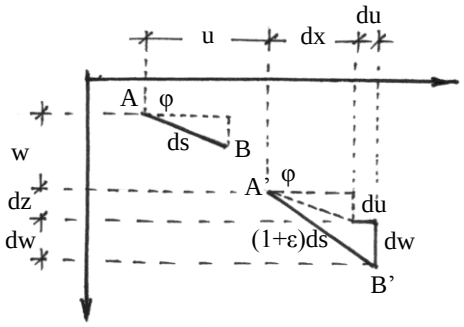

Figure 2. Deformation of an infinitesimal part ds

From the second of the above (2c) we obtain:

$$\int_0^L du = u(L) - u(0) = \int_0^L \varepsilon \cdot (1 + z'^2) dx - \int_0^L z' \cdot w' dx = 0$$

which after integration gives (because $w(0) = w(L) = u(0) = 0$):

$$\int_0^L \varepsilon \cdot (1 + z'^2) dx + \int_0^L z'' \cdot w dx = 0 \qquad (2d)$$

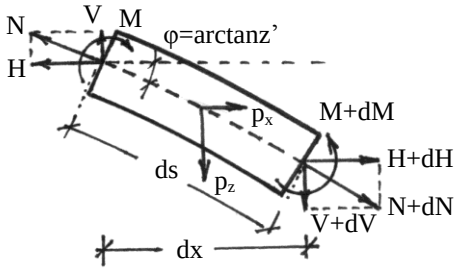

Figure 3. Equilibrium of an infinitesimal part ds

From figure 3 we get $dH = -p_x dx$ and because it is usually $p_x = 0$, we obtain:
On the other hand we know that:

$$\left.\begin{aligned} \varepsilon = \frac{N}{E \cdot A(x)}, \quad 1 + z'^2 = \frac{1}{\cos^2 \varphi}, \quad N = \frac{H}{\cos \varphi} \end{aligned}\right\} \qquad (2e)$$

Therefore, equation (2d) becomes:

$$\int_0^L \frac{N}{E \cdot A(x) \cdot \cos^2 \varphi} dx = \int_0^L \frac{H}{E \cdot A(x) \cdot \cos^3 \varphi} dx = -\int_0^L z'' \cdot w dx \qquad (2f)$$

$$H = \text{constant} \qquad (3a)$$

And thus:

$$\left.\begin{aligned} H &= -\frac{1}{K} \cdot \int_0^L z'' \cdot w dx \\ \text{where: } K &= \int_0^L \frac{dx}{EA(x) \cos^3 \varphi} \end{aligned}\right\} \qquad (3b)$$

From the equilibrium of figure 3 we conclude to the following equations:

$$z''H = -p_z\ ,\quad \frac{dV}{dx} = -p_z\ ,\quad \frac{d^2M}{dx^2} = H\cdot(z-w)'' + p_z \qquad \left.\right\} \tag{3c}$$

From the first of (2c) we get: $\frac{d\psi}{ds} = \frac{d^2w}{dx^2}\cdot\frac{dx}{ds} = -\frac{M}{EI_a}$ or $\frac{d^2w}{dx^2} = -\frac{M}{EI_a\cos\varphi}$

while because of (3c) and taking into account the inertia forces we obtain:

$$\frac{d^2}{dx^2}\left(EI_a\cos\varphi\frac{d^2w_a}{dx^2}\right) + H\cdot w_a'' + m_a\ddot{w}_a = p_z - \frac{z''}{K}\cdot\int_0^L z''\cdot w_a dx \tag{3d}$$

From equation (1) we find $z'' = 8f_o/L^2$ while we put, as usual, $I_a\cos\varphi = I_c$ where I_c is the moment of inertia at the top point of the arch. Therefore equation (3d) becomes:

$$EI_c w_a'''' - \frac{mgL^2}{8f_o}w_a'' + m_a\ddot{w}_a = p_z - \frac{64f_o^2}{KL^4}\int_0^L w_a dx \tag{3e}$$

Putting $p_z = 0$, we get the equation of the free motion from which we will try to determine the eigenfrequencies and the shape functions of the arch:

$$EI_c w_a'''' - \frac{mgL^2}{8f_o}w'' + m_a\ddot{w}_a = -\frac{64f_o^2}{KL^4}\int_0^L w_a dx \tag{4a}$$

We are searching for a solution of the form:

$$w_a(x,t) = W(x)\cdot e^{i\omega t} \tag{4b}$$

Therefore equation (4a) becomes:

$$\left.\begin{aligned} &W'''' - A\cdot W'' - k^4 W = -B\int_0^L W dx \\ &\text{where:}\quad A = \frac{mgL^2}{8f_o EI_c}\ ,\quad B = \frac{64\,f_o^2}{KL^4 EI_c}\ ,\quad k^4 = \frac{m_a\omega^2}{EI_c} \end{aligned}\right\} \tag{4c}$$

Given that the integral of the right site member is independent of x, the general solution of (4c) will be:

$$\left.\begin{aligned} &W(x) = c_1\sin\lambda_1 x + c_2\cos\lambda_1 x + c_3\,\mathrm{Sinh}\lambda_2 x + c_4\,\mathrm{Cosh}\lambda_2 x + \frac{B}{k^4}\int_0^L W dx \\ &\text{with:}\quad \lambda_1 = \sqrt{-\frac{A}{2} + \sqrt{\frac{A^2}{4} + k^4}}\ ,\quad \lambda_2 = \sqrt{\frac{A}{2} + \sqrt{\frac{A^2}{4} + k^4}} \end{aligned}\right\} \tag{4d}$$

Integrating (4d) we find:

$$\int_0^L W dx = \frac{k^4}{k^4 - BL} \cdot \left[-\frac{c_1}{\lambda_1}(\cos\lambda_1 L - 1) + \frac{c_2}{\lambda_1}\sin\lambda_1 L + \frac{c_3}{\lambda_2}(\mathrm{Cosh}\lambda_2 L - 1) + \frac{c_4}{\lambda_2}\mathrm{Sinh}\lambda_2 L \right]$$

Therefore the final solution of equation (4c) becomes:

$$\left.\begin{aligned} W(x) = c_1\left[\sin\lambda_1 x - \frac{B}{\lambda_1(k^4 - BL)}(\cos\lambda_1 L - 1)\right] + c_2\left[\cos\lambda_1 x + \frac{B}{\lambda_1(k^4 - BL)}\sin\lambda_1 L\right] \\ + c_3\left[\mathrm{Sinh}\,\lambda_2 x + \frac{B}{\lambda_2(k^4 - BL)}(\mathrm{Cosh}\,\lambda_2 L - 1)\right] + c_4\left[\mathrm{Cosh}\,\lambda_2 x + \frac{B}{\lambda_2(k^4 - BL)}\mathrm{Sinh}\,\lambda_2 L\right] \end{aligned}\right\} \quad (4e)$$

With boundary conditions $W(0) = W(L) = W''(0) = W''(L) = 0$, we obtain the following equation for eigenfrequencies:

$$\begin{vmatrix} -\frac{B}{\lambda_1(k^4 - BL)}(\cos\lambda_1 L - 1) & \left(1 + \frac{B}{\lambda_1(k^4 - BL)}\sin\lambda_1 L\right) & \frac{B}{\lambda_2(k^4 - BL)}(\mathrm{Cosh}\,\lambda_2 L - 1) & \left(1 + \frac{B}{\lambda_2(k^4 - BL)}\mathrm{Sinh}\,\lambda_2 L\right) \\ \sin\lambda_1 L & \cos\lambda_1 L - 1 & \mathrm{Sinh}\lambda_2 L & \mathrm{Cosh}\lambda_2 L - 1 \\ 0 & -\lambda_1^2 & 0 & \lambda_2^2 \\ -\lambda_1^2 \sin\lambda_1 L & -\lambda_1^2 \cos\lambda_1 L & \lambda_2^2 \mathrm{Sinh}\,\lambda_2 L & \lambda_2^2 \mathrm{Cosh}\,\lambda_2 L \end{vmatrix} = 0$$

(5a)

Finally the shape functions are given by (4e) with:

$$\left.\begin{aligned} c_2 &= -c_1 \cdot \frac{\sin\lambda_1 L}{\cos\lambda_1 L - 1} \\ c_3 &= c_1 \cdot \left(\frac{\lambda_1}{\lambda_2}\right)^2 \cdot \frac{\sin\lambda_1 L \cdot (\mathrm{Cosh}\lambda_2 L - 1)}{\mathrm{Sinh}\lambda_2 L \cdot (\cos\lambda_1 L - 1)} \\ c_4 &= -c_1 \cdot \left(\frac{\lambda_1}{\lambda_2}\right)^2 \cdot \frac{\sin\lambda_1 L}{\cos\lambda_1 L - 1} \end{aligned}\right\} \quad (5b)$$

2.2. The deck

The deck of figure 4 has the following equation of motion:

$$EI_d w_d'''' + m\ddot{w}_d = p_z \quad (6a)$$

The shape functions are:

$$Z_n = \sin\frac{n\pi x}{L} \tag{6b}$$

and its eigenfrequencies are given by the formula:

$$\omega_{dn} = \sqrt{\frac{n^4\pi^4 E I_d}{m_d L^4}} \tag{6c}$$

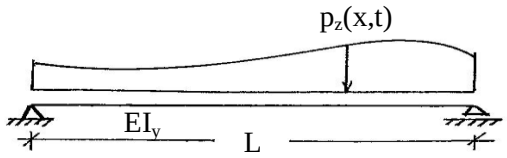

Figure 4. The deck

2.3 The cables

We consider a suspended arch bridge with two lines of cables.

It is valid that: $\sigma = \frac{q_z}{2A_c} = \varepsilon E_c = \frac{\Delta\ell}{\ell}\cdot E_c = \frac{w_d - w_a}{\ell}\cdot E_c$ which concludes to the following expression:

$$q_z(x,t) = \frac{2E_c A_c}{z(x)}\cdot(w_d - w_a) \tag{7}$$

Where A_c is the area of the one line of the cables' cross-section per unit length of the deck and E_c is the modulus of elasticity of the cables.

3 THE 2D MODEL

Let us consider now the suspended arch bridge shown in figure 5.
The following equations are valid:
For the arch

$$E I_c w_a'''' - \frac{m_a g L^2}{8 f_o}\cdot w_a'' + c\dot{w}_a + m_a\ddot{w}_a = q_z(x,t) - \frac{64 f_o}{K L^4}\cdot\int_0^L w_a dx \tag{8a}$$

And for the deck

$$EI_d w_d'''' + c\cdot\dot{w}_d + m\ddot{w}_d = p_z(x,t) - q_z(x,t) \tag{8b}$$

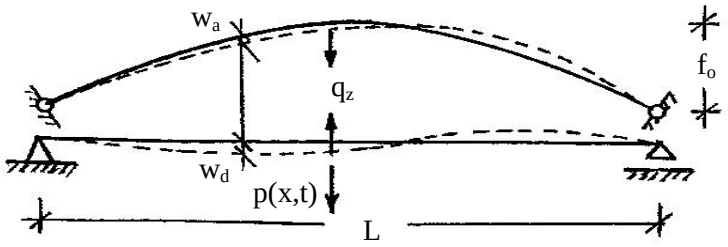

Figure 5. The suspended arch bridge

Introducing $q_z(x,t)$ from equation (7) into equations (8a,b) we get:

$$\left.\begin{aligned} EI_c w_a'''' - \frac{m_a g L^2}{8 f_o}\cdot w_a'' + \frac{2E_c A_c}{z(x)} w_a + c\dot{w}_a + m_a \ddot{w}_a &= \frac{2E_c A_c}{z(x)} w_d - \frac{64 f_o}{KL^4}\cdot \int_0^L w_a dx \\ EI_d w_d'''' + \frac{2E_c A_c}{z(x)} w_d + c\cdot \dot{w}_d + m\ddot{w}_d &= p_z(x,t) + \frac{2E_c A_c}{z(x)} w_a \end{aligned}\right\} \quad (9a,b)$$

We are searching for a solution of the form:

$$\left.\begin{aligned} w_a(x,t) &= \sum_n W_n(x)\cdot T_n(t) \\ w_d(x,t) &= \sum_n Z_n(x)\cdot R_n(t) \end{aligned}\right\} \quad (10a,b)$$

where W_n from equation (4e) and Z_n from equation (6b), are the shape functions of the arch and the deck respectively, while T_n and R_n are time functions under determination.

Introducing the above expressions into equations (9a,b) we obtain:

$$\left.\begin{aligned} EI_c \sum_n W_n'''' T_n - \frac{m_a g L^2}{8 f_o}\sum_n W_n'' T_n + \frac{2E_c A_c}{z(x)}\sum_n W_n T_n + c\sum_n W_n \dot{T}_n + m_a \sum_n W_n \ddot{T}_n = \\ = \frac{2E_c A_c}{z(x)}\sum_n Z_n R_n - \frac{64 f_o^2}{KL^4}\int_0^L \sum_n W_n T_n dx \\ EI_d \sum_n Z_n'''' R_n + \frac{2E_c A_c}{z(x)}\sum_n Z_n R_n + c\sum_n Z_n \dot{R}_n + m_d \sum_n Z_n \ddot{R}_n = p_z(x,t) + \frac{2E_c A_c}{z(x)}\sum_n W_n T_n \end{aligned}\right\} \quad (11a,b)$$

We remember that W_n and Z_n satisfy the following equations of the free motion:

$$\left.\begin{aligned} &E\,I_c W_n'''' - \frac{mgL^2}{8f_o} W_n'' + m_a \omega_{an}^2 W_n = -\frac{64 f_o^2}{KL^4} \int_0^L W_n\,dx \\ &E\,I_d Z_n'''' - m_d \omega_{dn}^2 Z_n = 0 \end{aligned}\right\}$$

Therefore equations (11a,b) become:

$$\left.\begin{aligned} &m_a \sum_n W_n \ddot{T}_n + c \sum_n W_n \dot{T}_n + m_a \sum_n \omega_{an}^2 W_n T_n + \frac{2E_c A_c}{z(x)} \sum_n W_n T_n - \frac{2E_c A_c}{z(x)} \sum_n Z_n R_n = 0 \\ &m_d \sum_n Z_n \ddot{R}_n + c \cdot \sum_n Z_n \dot{R}_n + m_d \sum_n \omega_{dn}^2 Z_n R_n + \frac{2E_c A_c}{z(x)} \sum_n Z_n R_n - \frac{2E_c A_c}{z(x)} \sum_n W_n T_n = p_z(x,t) \end{aligned}\right\} \quad (12a,b)$$

Multiplying the first of (12) by W_ρ and integrating, the second of (12) by Z_ρ and integrating and taking into account the orthogonality conditions, we finally find:

$$\left.\begin{aligned} &\ddot{T}_\rho + \frac{c}{m_a} \dot{T}_\rho + \omega_{a\rho}^2 T_\rho + \Gamma_\rho \sum_n \left(T_n \int_0^L \frac{W_n W_\rho}{z(x)} dx \right) - \Gamma_\rho \sum_n \left(R_n \int_0^L \frac{Z_n W_\rho}{z(x)} dx \right) = 0 \\ &\ddot{R}_\rho + \frac{c}{m_d} \dot{R}_\rho + \omega_{d\rho}^2 R_\rho + \Delta_\rho \sum_n \left(R_n \int_0^L \frac{Z_n Z_\rho}{z(x)} dx \right) - \Delta_\rho \sum_n \left(T_n \int_0^L \frac{W_n Z_\rho}{z(x)} dx \right) = \frac{1}{m_d \int_0^L Z_\rho^2 dx} \int_0^L p_z Z_\rho dx \end{aligned}\right\} \quad (13a,b)$$

Without restriction of the generality, one can suppose that the following is valid:

$$p_z(x,t) = p_z(x) \cdot f_z(t) \quad (14)$$

In order to solve the system (13) we use the Laplace transformation, with initial conditions $R_\rho(0) = \dot{R}_\rho(0) = T_\rho(0) = \dot{T}_\rho(0) = 0$. We put:

$$\left.\begin{aligned} &L T_\rho(t) = \overline{T}_\rho(s), \qquad L R_\rho(t) = L\overline{R}_\rho(s) \\ &L \dot{T}_\rho(t) = s \cdot \overline{T}_\rho(s), \quad L \dot{R}_\rho(t) = s \cdot \overline{R}_\rho(s) \\ &L \ddot{T}_\rho(t) = s^2 \cdot \overline{T}_\rho(s), \quad L \ddot{R}_\rho(t) = s^2 \cdot \overline{R}_\rho(s) \\ &L f_z(t) = \bar{f}_z(s) \end{aligned}\right\} \quad (15)$$

And also:

$$\left.\begin{aligned}
&\alpha_{n\rho} = \Gamma_\rho \int_0^L \frac{W_n W_\rho}{z(x)}\,dx\,, \quad \beta_{n\rho} = \Gamma_\rho \int_0^L \frac{Z_n W_\rho}{z(x)}\,dx \\
&\gamma_{n\rho} = \Delta_\rho \int_0^L \frac{Z_n Z_\rho}{z(x)}\,dx\,, \quad \delta_{n\rho} = \Delta_\rho \int_0^L \frac{W_n Z_\rho}{z(x)}\,dx \\
&\varepsilon_\rho = \frac{\Delta_\rho}{2E_c A_c} \int_0^L p_z(x)\cdot Z_\rho\,dx
\end{aligned}\right\} \qquad (16)$$

Introducing the above equations (15) and (16) into (13) we obtain the following linear system:

$$\left.\begin{aligned}
&\alpha_{1\rho}\overline{T}_1 + ... + (\alpha_{\rho\rho} + s^2 + \frac{c}{m_a}s + \omega_{\alpha\rho}^2)\overline{T}_\rho + ... + \alpha_{n\rho}\overline{T}_n - \beta_{1\rho}\overline{R}_1 - .... - \beta_{n\rho}\overline{R}_n = 0 \\
&\gamma_{1\rho}\overline{R}_1 + ... + (\gamma_{\rho\rho} + s^2 + \frac{c}{m_d}s + \omega_{d\rho}^2)\overline{R}_\rho + ... + \gamma_{n\rho}\overline{R}_n - \delta_{1\rho}\overline{T}_1 - .... - \delta_{n\rho}\overline{T}_n = \varepsilon\cdot\overline{f}_z
\end{aligned}\right\} \qquad (17a,b)$$

with ρ=1 to n.

Solving the above system we determine $\overline{T}_\rho$ and $\overline{R}_\rho$ and further:

$$\left.\begin{aligned}
T_\rho(t) &= L^{-1}\overline{T}_\rho(s) \\
R_\rho(t) &= L^{-1}\overline{R}_\rho(s)
\end{aligned}\right\} \qquad (18a,b)$$

4 THE 3D MODEL

Let us consider now a 3D model, whose the cross-section and the sign convention of deformations and of the cables' stresses are shown in figure 6.

We accept the following:

1. The arch and the deck have the same width 2b
2. We suppose that both arch and deck have non deformable cross-sections in their plan and therefore the motion of each one can be expressed by the displacement of their gravity center.
3. Angle φ_a is negligible.

The following relations are valid:

$$\left.\begin{aligned}
w_{\Gamma'} &= w_d + b\,\varphi_d \\
w_{\Delta'} &= w_d - b\,\varphi_d
\end{aligned}\right\} \qquad (19a)$$

Therefore from equation (7) we get:

$$\left.\begin{aligned} q_1 &= \frac{E_c A_c}{z(x)}(w_d - w_a + b\varphi_d) \\ q_2 &= \frac{E_c A_c}{z(x)}(w_d - w_a - b\varphi_d) \end{aligned}\right\} \tag{19b}$$

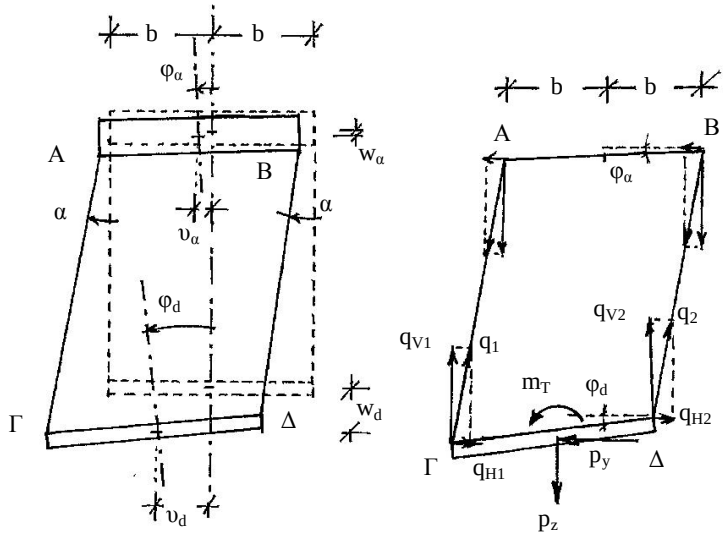

Figure 6. The 3D problem. Deformations and Stresses

From equations (19b) we obtain:

$$\left.\begin{aligned} q_1 + q_2 &= \frac{E_c A_c}{z(x)}(w_d - w_a) \\ q_1 - q_2 &= \frac{E_c A_c}{z(x)} \cdot b\varphi_d \end{aligned}\right\} \tag{19c}$$

On the other hand because the angle α is very small we have:

$$\left.\begin{aligned} q_{V1} + q_{V2} &= q_1 + q_2 \\ q_{H1} + q_{H2} &= (q_1 + q_2) \cdot \frac{\upsilon_d}{z(x)} \\ q_{H1} - q_{H2} &= (q_1 - q_2) \cdot \frac{\upsilon_d}{z(x)} \end{aligned}\right\} \tag{19d}$$

The equations of the problem are the following:

For the deck

$$\left.\begin{aligned} &E I_y w_d'''' + c\dot{w}_d + m_d \ddot{w}_d = p_z - (q_1 + q_2) \\ &E I_z \upsilon_d'''' + c\dot{\upsilon}_d + m_d \ddot{\upsilon}_d = p_y - (q_1 - q_2)\cdot \frac{\upsilon_d}{z(x)} \\ &E I_\omega \varphi_d'''' - G I_D \varphi_d'' + c\dot{\varphi}_d + J_{px}\ddot{\varphi}_d = m_x - (q_1 - q_2)\cdot b - (q_1 - q_2)\cdot \frac{\upsilon_d}{z(x)}\cdot b\cdot \varphi_d \end{aligned}\right\}$$

For the arch

$$\left.\begin{aligned} &E I_c w_a'''' - \frac{m_a g L^2}{8 f_o} w_a'' + c\dot{w}_a + m_a \ddot{w}_a = (q_1 + q_2) - \frac{64 f_o^2}{K L^4}\int_0^L w_a dx \\ &E I_{za}(\upsilon_a'''' + \frac{\varphi_a''}{R}) + c\dot{\upsilon}_a + m_a \ddot{\upsilon}_a = (q_{H1} - q_{H2}) \end{aligned}\right\}$$

The above two sets of equations, because of equations (19), and neglecting the higher order terms like $(\upsilon_d \cdot \varphi_d)$, become:

For the deck

$$\left.\begin{aligned} &E I_y w_d'''' + \frac{2E_c A_c}{z(x)} w_d + c\dot{w}_d + m_d \ddot{w}_d = p_z(x,t) + \frac{2E_c A_c}{z(x)} w_a \\ &E I_z \upsilon_d'''' + c\dot{\upsilon}_d + m_d \ddot{\upsilon}_d = p_y(x,t) - \frac{2E_c A_c}{z(x)}(w_d - w_a)\cdot \frac{\upsilon_d}{z(x)} \\ &E I_\omega \varphi_d'''' - G I_D \varphi_d'' + c\dot{\varphi}_d + J_{px}\ddot{\varphi}_d = m_x(x,t) - \frac{2E_c A_c}{z(x)}\cdot b^2 \cdot \varphi_d \end{aligned}\right\} \quad (20a,b,c)$$

For the arch

$$\left.\begin{aligned} &E I_c w_a'''' - \frac{m_a g L^2}{8 f_o} w_a'' + \frac{2E_c A_c}{z(x)} w_a + c\dot{w}_a + m_a \ddot{w}_a = \frac{2E_c A_c}{z(x)} w_d - \frac{64 f_o^2}{K L^4}\int_0^L w_a dx \\ &E I_{za}\upsilon_a'''' + c\dot{\upsilon}_a + m_a \ddot{\upsilon}_a = \frac{2E_c A_c}{z(x)}(w_d - w_a)\frac{\upsilon_d}{z(x)} \end{aligned}\right\} (21a,b)$$

In order to solve the above complicated system of equations (20) and (21) we follow the following steps:

1st Step

The system of equations (20a) and (21a) are exactly the equations(9a,b) and therefore their solution is given in §3 (equations (16), (17) and (18)).

2nd Step

In order to solve equation (20c), we are searching for a solution of the form:

$$\varphi_d(x,t) = \sum_n \Phi_n(x) \cdot U_n(t) \tag{22a}$$

where $\Phi_n(x)$ are the shape functions of a single beam in torsion (given by equation 22b) and $U_n(t)$ the time function under determination.

$$\left.\begin{aligned} \Phi_n(x) &= \sin\lambda_{1n}x - \frac{\sin\lambda_{1n}L}{\sinh\lambda_{2n}L}\cdot\sinh\lambda_{2n}x \\ \text{with:}\quad \lambda_{1n} &= \sqrt{-\frac{GI_D}{2EI\omega} + \sqrt{\left(\frac{GI_D}{2EI\omega}\right)^2 + \frac{J_{px}\omega_{\varphi n}^2}{EI_\omega}}} \\ \lambda_{1n} &= \sqrt{\frac{GI_D}{2EI\omega} + \sqrt{\left(\frac{GI_D}{2EI\omega}\right)^2 + \frac{J_{px}\omega_{\varphi n}^2}{EI_\omega}}} \\ \text{and:}\quad \omega_{\varphi n}^2 &= \frac{n^4\pi^4 EI_\omega}{J_{px}L^4} + \frac{n^2\pi^2 GI_D}{J_{px}L^2} \end{aligned}\right\} \tag{22b}$$

Introducing (22a) into equation (20c) we get:

$$EI_\omega\sum_n \Phi_n'''U_n - GI_D\sum_n \Phi_n''U_n + c\sum_n \Phi_n\dot{U}_n + J_{px}\sum_n \Phi_n\ddot{U}_n =$$
$$= m_x(x,t) - \frac{2E_cA_c}{z(x)}b^2\sum_n \Phi_nU_n$$

Taking into account that $\Phi_n(x)$ satisfies the equation of free motion the above becomes:

$$J_{px}\sum_n \omega_{\varphi n}^2\Phi_nU_n + c\sum_n \Phi_n\dot{U}_n + J_{px}\sum_n \Phi_n\ddot{U}_n = m_x(x,t) - \frac{2E_cA_c}{z(x)}b^2\sum_n \Phi_nU_n$$

Multiplying the above by $\Phi_\rho(x)$, integrating from 0 to L and taking into account the orthogonality conditions we conclude to the following equation:

$$\ddot{U}_\rho + \frac{c}{J_{px}}\dot{U}_\rho + \omega_{\varphi\rho}^2U_\rho = \frac{\int_0^L m_x(x,t)\Phi_\rho dx}{J_{px}\cdot\int_0^L \Phi_\rho^2 dx} - \frac{2b^2E_cA_c}{J_{px}\cdot\int_0^L \Phi_\rho^2 dx}\sum_n\left(U_n\int_0^L \frac{\Phi_n\Phi_\rho}{z(x)}dx\right) \tag{23a}$$

Without restriction of the generality we put

$$m_x(x,t) = m_x(x)\cdot f_x(t) \tag{23b}$$

In order to solve the system (23a), we use the Lagrange transformation and

with initial conditions $U_\rho(0) = \dot{U}_\rho(0) = 0$ we put:

$$\left.\begin{aligned} &LU_\rho(t) = \overline{U}_\rho(s)\,, \quad Lf_x(t) = \bar{f}_x(s) \\ &L\dot{U}_\rho(t) = s\overline{U}_\rho(s)\,, \quad L\ddot{U}_\rho(t) = s^2\overline{U}_\rho(s) \end{aligned}\right\} \tag{23c}$$

and also

$$\left.\begin{aligned} \zeta_{n\rho} &= \frac{2b^2 E_c A_c}{J_{px}} \cdot \frac{\int_0^L \frac{\Phi_n \Phi_\rho}{z(x)}\,dx}{\int_0^L \Phi_\rho^2\,dx}\,, \quad \xi_\rho = \frac{\int_0^L m_x(x)\Phi_\rho\,dx}{J_{px}\int_0^L \Phi_\rho^2\,dx} \end{aligned}\right\} \tag{23d}$$

Introducing the above into (23a) we obtain:

$$\zeta_{1\rho}\overline{U}_1 + ...+ (\zeta_{\rho\rho} + s^2 + \frac{c}{J_{px}}\cdot s + \omega_{\varphi\rho}^2)\overline{U}_\rho + ...+ \zeta_{n\rho}\overline{U}_n = \xi_\rho \cdot \bar{f}_x(s) \tag{24a}$$

with ρ=1 to n.

Solving the above system we determine the $\overline{U}_\rho(s)$ and further:

$$U_\rho(t) = L^{-1}\overline{U}_\rho(s) \tag{24b}$$

3rd Step

We observe that equation (20b) is a non-linear differential equation, which, obviously, can not be solved by classical elementary methods. Therefore we will try to achieve an approximate solution by applying the method exposed in [31, 32].

Neglecting for instant the non-linear terms we get the equation:

$$EI_z\upsilon_d'''' + c\dot{\upsilon}_d + m_d\ddot{\upsilon}_d = p_y(x)\cdot f_y(t)$$

and following the well known procedure we obtain the solution:

$$\left.\begin{aligned} &\upsilon_d(x,t) = \sum_n \sin\frac{n\pi x}{L}\cdot G_n(t) \\ &\text{with} \quad G_n(t) = \frac{2\int_0^L p_y(x)\cdot\sin\frac{n\pi x}{L}\,dx}{m_d\cdot L\cdot\overline{\omega}_{\upsilon n}}\cdot\int_0^t f_y(\tau)\cdot e^{-\beta(t-\tau)}\sin\overline{\omega}_{\upsilon n}(t-\tau)\,d\tau \\ &\text{and:} \quad \beta = \frac{c}{2m_d}\,, \quad \overline{\omega}_{\upsilon n} = \sqrt{\omega_{\upsilon n}^2 - \beta^2}\,, \quad \omega_{\upsilon n}^2 = \frac{n^4\pi^4 EI_z}{m_d L^4} \end{aligned}\right\} \tag{25}$$

Knowing w_d and w_a from the solution of the first step and υ_d from the first of equation (25) we get the function:

$$\Xi(x,t) = -\frac{2E_cA_c}{z(x)}(w_d - w_a)\frac{\upsilon_d}{z(x)} = -\frac{2E_cA_c}{z(x)}\sum_n [W_n(x)T_n(t) - Z_n(x)R_n(t)]\cdot\sum_n \sin\frac{n\pi x}{L}\cdot U_n(t) \tag{26a}$$

Considering now equation (20b) with the right side member having only the non-linear terms, we get the equation: $EI_z\upsilon_d'''' + c\dot{\upsilon}_d + m_d\ddot{\upsilon}_d = \Xi(x,t)$, which has the solution

$$\left.\begin{aligned} &\upsilon_d = \sum_n \sin\frac{n\pi x}{L}\cdot\Omega_n(t), \quad \text{with} \\ &\Omega_n(t) = \frac{2}{m_d\cdot\overline{\omega}_{\varphi n}\cdot L}\cdot\int_0^t\left(\int_0^L \Xi(x,\tau)\cdot\sin\frac{n\pi x}{L}dx\right)\cdot e^{-\beta(t-\tau)}\sin\overline{\omega}_{\varphi n}(t-\tau)d\tau \end{aligned}\right\} \tag{26b}$$

Therefore the complete solution of equation (20b) will be:

$$\upsilon_d(x,t) = \sum_n \sin\frac{n\pi x}{L}\cdot[G_n(t) - \Omega_n(t)] \tag{26c}$$

4th Step

Equation (21b) has exactly the same form with equation (20b) and therefore it is solved -4

5 NUMERICAL EXAMPLES AND DISCUSSION

Let us consider us a suspended arch bridge like the one of figure 5.

The bridge is made for isotropic homogeneous material with modulus of elasticity $E_s = 2.1\cdot10^8\,kN/m^2$ and shear modulus $G = 0.8\cdot10^8\,kN/m^2$.

The length of the bridge is $L = 120m$ and its width $2b = 10m$.

For the arch we have $f_o = 18m$, $I_c = 0.2\,m^4$ and $m_a = 300kg/m$.

For the deck we have moments of inertia in bending $I_y = 0.03m^4$, $I_z = 0.10m^4$, torsional moment of inertia $I_D = 0.01\cdot10^{-2}\,m^4$, warping resistance $I_\omega = 1.2\,m^6$, rotational mass moment of inertia $I_{px} = 26kNmsec^2$, and mass per unit length $m_d = 200kg/m$.

The cables are placed in tow rows at the edge of the cross-section of the bridge having area per unit step $A_c = 3.0\cdot10^{-4}\,m^2/m/row$, and modulus of

elasticity $E_c = 1.5 \cdot 10^8 \, kN/m^2$.

An initial elevation has been given to the deck by prestressing of the cables according to the following expression: $\upsilon_{do} = 0.001 \cdot \sin \frac{\pi x}{L}$.

At t=0, a moving concentrated load F=600 kN or a distributed one p=20 kN/m^2 enters the bridge moving with velocity v, and acting centrically or eccentrically.

3.1 The 2D model

A. The moving concentrated load.

Considering firstly a concentrated load of F=600 kN moving on the axis of the deck with constant velocity v=20 m/sec (or else 72 km/h) and applying the formulae of §3 we obtain the following plots of figures 7 and 8.

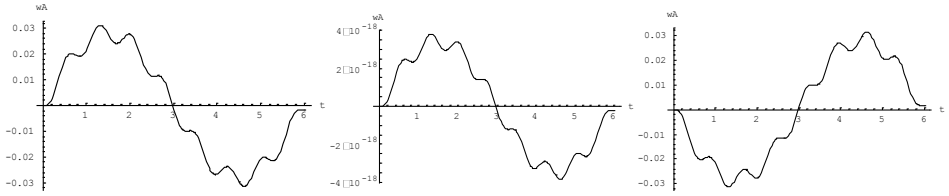

x=L/4 x=L/2 x=3L/4

Figure 7. The motion of the arch's first quarter, middle, and third quarter

From the above plots, we verify that always the arch is deformed in anti symmetrical forms which the middle point has negligible motion.

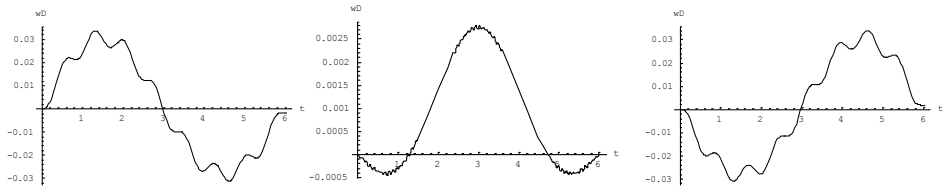

x=L/4 x=L/2 x=3L/4

Figure 8. The motion of the deck's first quarter, middle, and third quarter

The motion of the deck's first quarter, middle and third quarter are shown in figure 8, while the tensions of the cables are shown in figure 9 for different time instants.

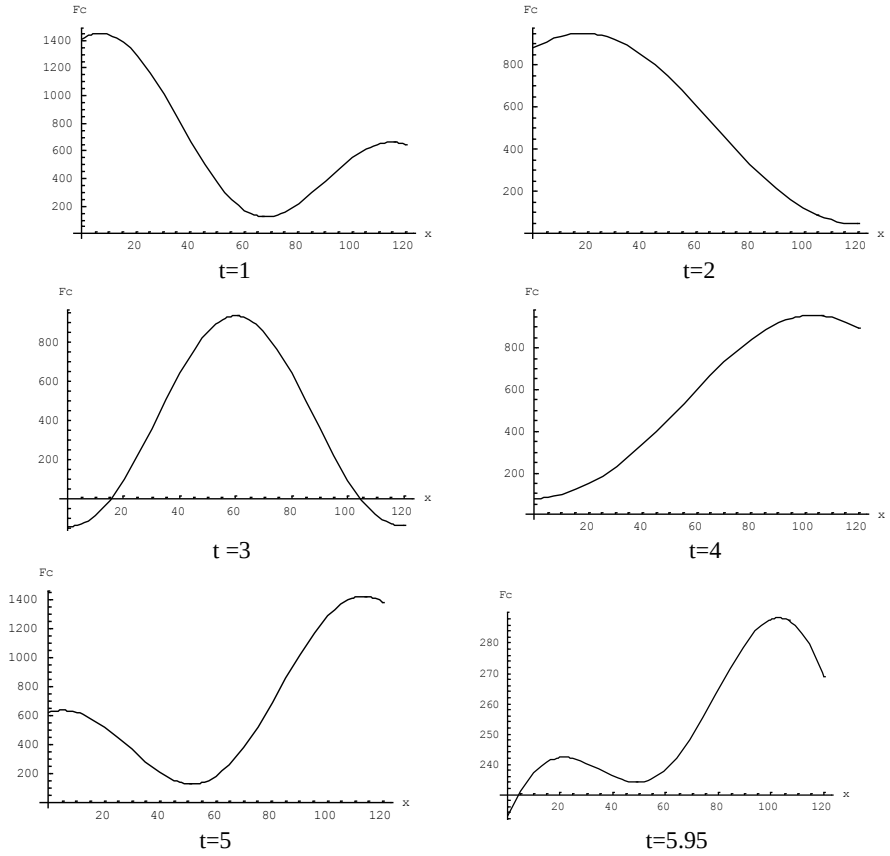

Figure 9. The cables forces at different time instants

B. The moving distributed load.

Considering now a distributed load of p=20 kN/m^2, acting on a width of 2 meters, moving on the axis of the deck with constant velocity v=20 m/sec (or else 72 km/h) and applying the formulae of §3 we obtain the following plots of figures 10, 11 and 12.

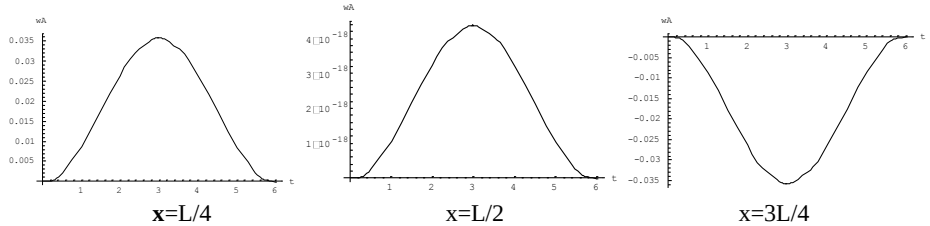

Figure 10. The motion of the arch's first quarter, middle, and third quarter

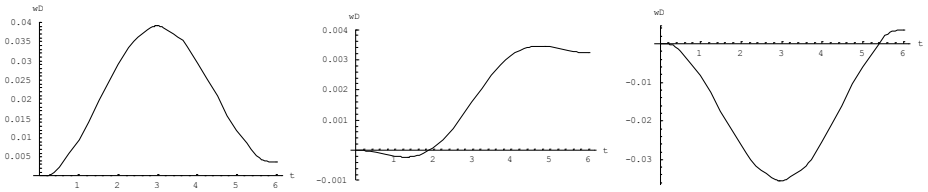

Figure 11. The motion of the deck's first quarter, middle, and third quarter

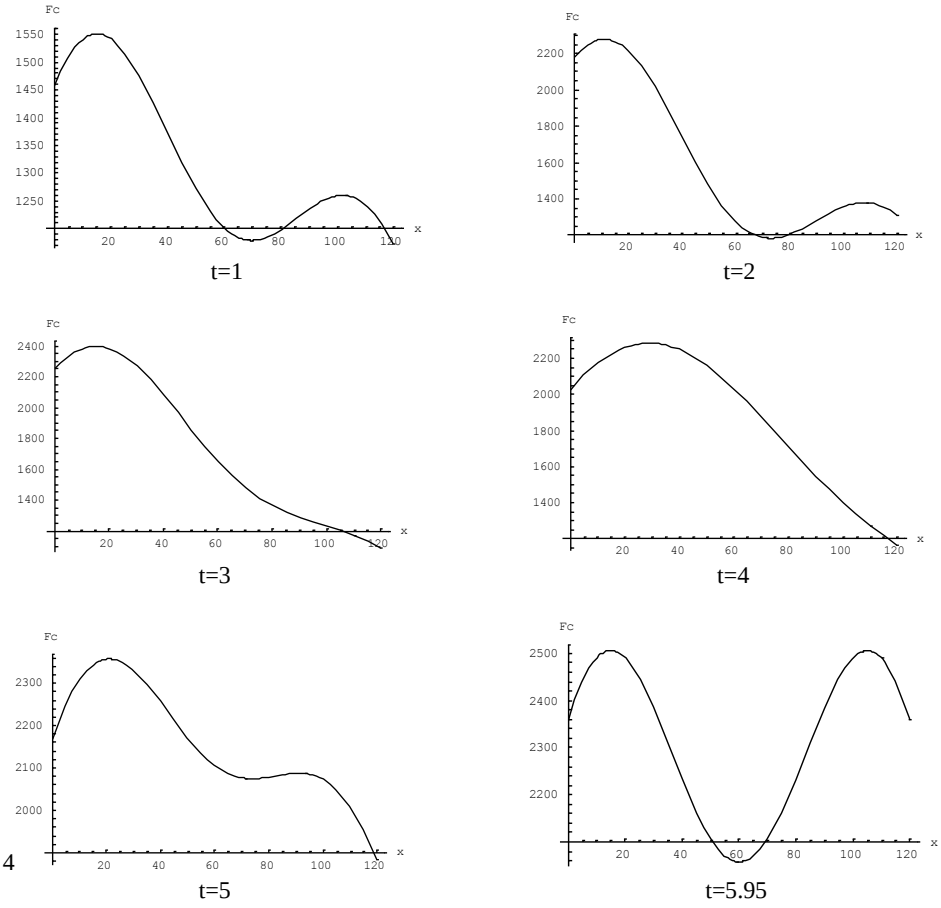

Figure 12. The cables forces at different time instants

3.2 The 3D model

A. The moving concentrated load.

We consider now that the above in §3.1.A concentrated load moves on the deck eccentrically with eccentricity e=1 m. Therefore the bridge oscillates with a torsional motion which can be determined applying the formulae of §4 (step 2).

The so produced angles φ along the deck are shown in figure 13 for different time instants.

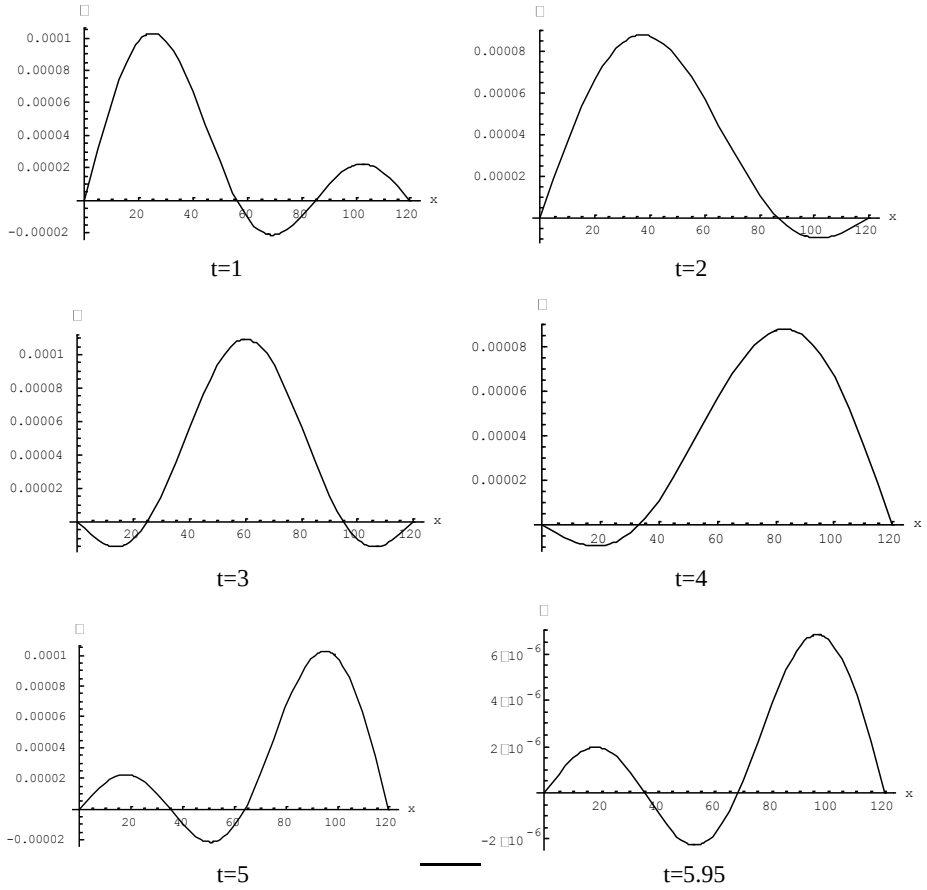

Figure 13. The angle φ of the deck motion for different time instants

Finally the cables' forces of the tow row of cables are shown in the plots of the next figure 14.

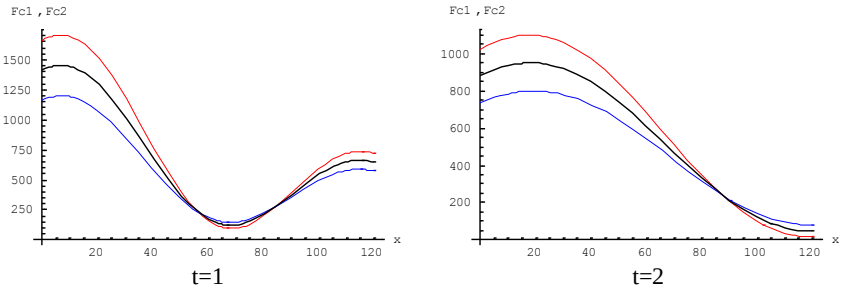

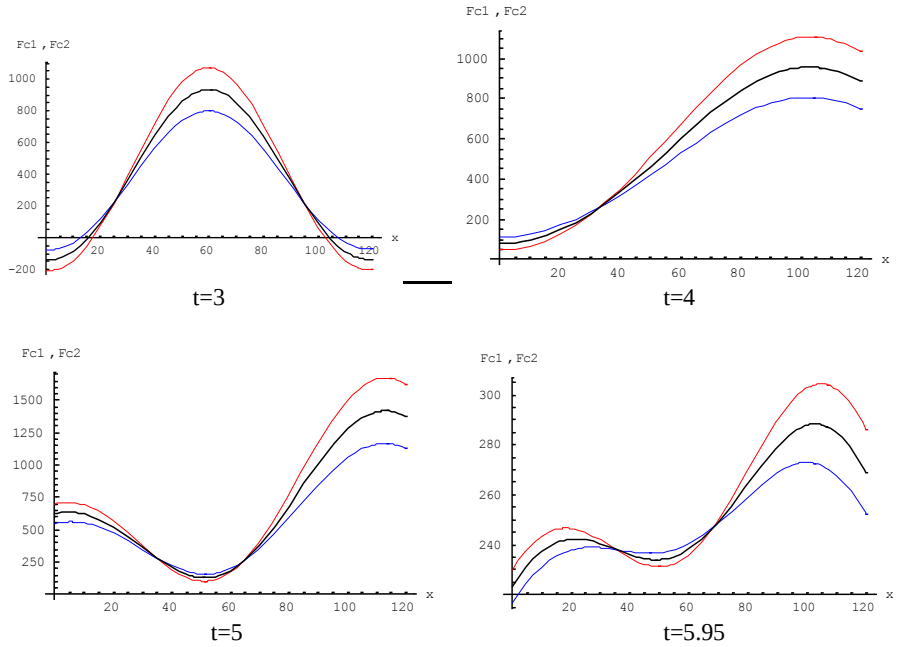

Figure 14. The cables forces at different time instant. black: cables forces with load acting centrically, red: forces of the left row of cables, blue: forces of the right row of cables

We see, as was expected, that the left row of cables is charged more than the right one as the load acts nearest to the left row of cables.

B. The moving distributed load.

We consider now that the above in §3.1.B distributed load moves on the deck eccentrically with eccentricity e=4 m. Therefore the bridge oscillates with a torsional motion which can be determined applying the formulae of §4 (step 2). The so produced angles φ along the deck are shown in figure 15 for different time instants.

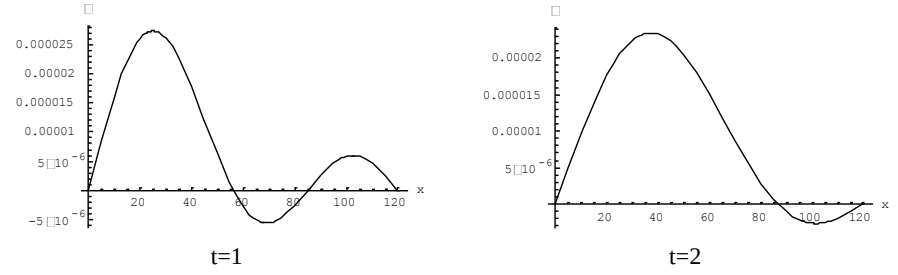

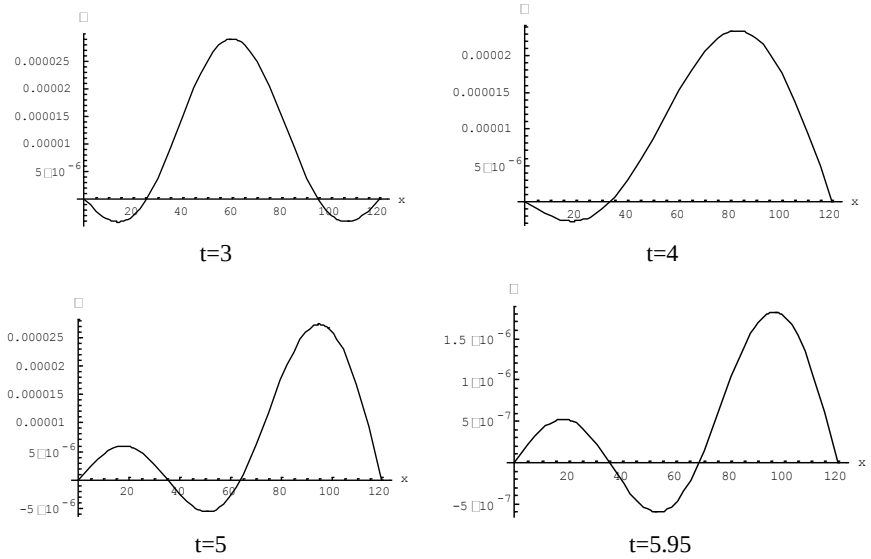

Figure 15. The angle φ of the deck motion for different time instants

Finally the cables' forces of the tow row of cables are shown in the plots of the next figure 16.

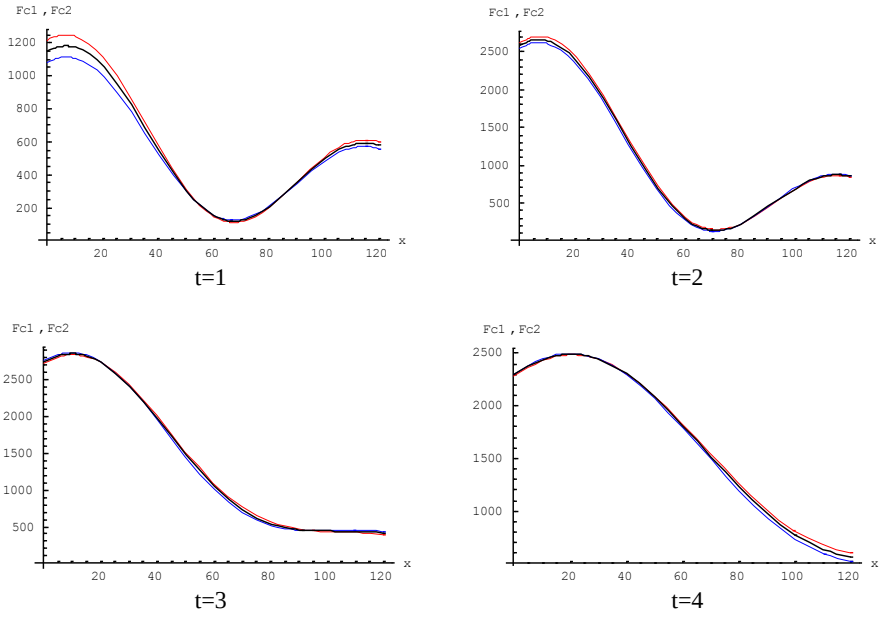

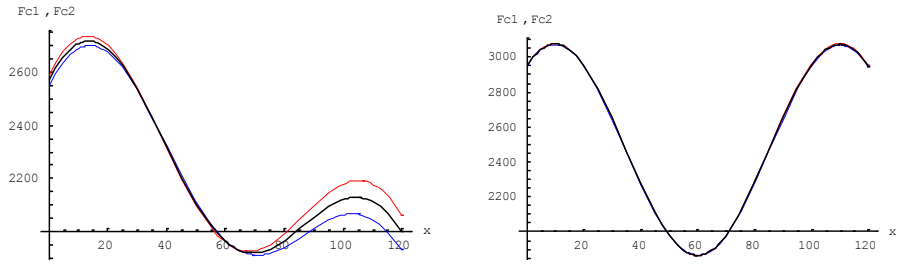

Figure 16. The cables forces at different time instant. black: cables forces with load acting centrically, red: forces of the left row of cables, blue: forces of the right row of cables

We see, as was expected, that the left row of cables is charged more than the right one as the load acts nearest to the left row of cables.

6. CONCLUSIONS

From the results of the model considered, one can draw the following conclusions.

1. A mathematical model is proposed either for the 2D distress and for the 3D distress of the bridge. The above models with densely placed cables can also be easily applied for sparse cables installation.
2. The specific behavior of the arch, which is always deformed into anti symmetrical shapes, has been verified, while its midpoint at x=L/2 remains practically immovable having negligible motion, as one can be seen in figures 7 and 10.
3. Although the total distributed load is less than the concentrated one, it causes greater tensions on the cables, perhaps because it acts, each time, on a larger part of the deck.
4. The eccentrically moving concentrated load causes a greater difference in cables tensions of each row even if it acts at a relatively smaller eccentricity than the distributed one, showing that the concentrated loads or vehicles are more dangerous.
5. Both concentrated or distributed moving loads cause the largest stressing of the cables and the greatest difference between the stressing of the two rows of cables when entering or exiting the bridge.

REFERENCES

[1] Johnston B.G. “Guide to stability design criteria for metal structures”, Structural Stability Research Council, 3rd edition, John Wiley & Sons, N.Y., 1976.

[2] Bergmeister, K., Capsoni, A., Corradi, L., Menardo, A. “Lateral elastic stability of slender arches for bridges including deck slenderness”, Structural Engineering International: Journal of the International Association for Bridge and Structural Engineering (IABSE), 19 (2), pp. 149-154, 2009.

[3] Pircher, M., Stacha, M., Wagner, J. "Stability of network arch bridges under traffic loading”

Proceedings of the Institution of Civil Engineers: Bridge Engineering 166 (3), pp. 186-192, 2013.
[4] Wang, Y., Liu, C., Liang, Y., Zhang, S. "Nonlinear stability analysis and completed bridge test on slanting type CFST arch bridges", Source of the Document Jianzhu Jiegou Xuebao/Journal of Building Structures 36, pp. 107-113, 2015.
[5] Zhu, X.-L., Sun, D.-B. "Nonlinear in-plane stability and catastrophe analysis of shallow arches", Zhendong yu Chongji/Journal of Vibration and Shock 35 (6), pp. 47-51 and 74, 2016.
[6] Bruno, D., Lonetti, P., Pascuzzo, A. "Document An optimization model for the design of network arch bridges", Computers and Structures 170, pp. 13-25, 2016.
[7] Mannini, C., Belloli, M., Marra, A.M., (...), Robustelli, F., Bartoli, G. "Aeroelastic stability of two long-span arch structures: A collaborative experience in two wind tunnel facilities", Engineering Structures 119, pp. 252-263, 2016.
[8] Zhang, Z.-C. "Creep analysis of long span concrete-filled steel tubular arch bridges", Gongcheng Lixue/Engineering Mechanics 24 (5), pp. 151-160, 2007
[9] Shao, X., Peng, J., Li, L., Yan, B., Hu, J. "Time-dependent behavior of concrete-filled steel tubular arch bridge", Journal of Bridge Engineering 15 (1), pp. 98-107, 2010
[10] Loghman, A., Ghorbanpour Arani, A., Shajari, A.R., Amir, S. "Time-dependent thermoelastic creep analysis of rotating disk made of Al-SiC composite", Archive of Applied Mechanics 81 (12), pp. 1853-1864, 2011
[11] Lai, X.-Y., Li, S.-Y., Chen, B.-C., "The influence of addictives on the creep of concrete-filled steel tube", Harbin Gongye Daxue Xuebao/Journal of Harbin Institute of Technology 44 (SUPPL.1), pp. 248-251, 2012
[12] Granata, M.F., Arici, M. "Serviceability of segmental concrete arch-frame bridges built by cantilevering", Bridge Structures 9 (1), pp. 21-36, 2013
[13] Ma, Y.S., Wang, Y.F. "Creep effects on the reliability of a concrete-filled steel tube arch bridge", Journal of Bridge Engineering 18 (10), pp. 1095-1104, 2013
[14] Zhou, Y. "Concrete creep and thermal effects on the dynamic behavior of a concrete-filled steel tube arch bridge", Journal of Vibroengineering 16 (4), pp. 1735-1744, 2014
[15] Bradford, M.A., Pi, Y.-L. "Geometric Nonlinearity and Long-Term Behavior of Crown-Pinned CFST Arches", Journal of Structural Engineering (United States) 141 (8), 04014190, 2015.
[16] Li, J.-B., Ge, S.-J., Chen, H. "Document Seismic behavior analysis of a 5-span continuous half-through CFST arch bridge", World Information on Earthquake Engineering 21(3) pp110-115, 2005
[17] 17.Álvarez, J.J., Aparicio, A.C., Jara, J.M., Jara, M. "Seismic assessment of a long-span arch bridge considering the variation in axial forces induced by earthquakes", Engineering Structures 34, pp. 69-80, 2012
[18] Huang, F.-Y., Chen, B.-C., Li, J.-Z., Cheng, H.-D. "Shaking tables testing of concrete filled steel tubular single arch rib model under the excitation of rare earthquakes", Gongcheng Lixue/Engineering Mechanics 32 (7), pp. 64-73, 2015
[19] Sevim, B., Atamturktur, S., Altunişik, A.C., Bayraktar, A. "Ambient vibration testing and seismic behavior of historical arch bridges under near and far fault ground motions", Bulletin of Earthquake Engineering , 14(1), 241-259, 2016
[20] Lei, S., Gao, Y., Pan, D. "An optimization solution of Rayleigh damping coefficients on arch bridges with closely-spaced natural frequencies subjected to seismic excitations", Harbin Gongye Daxue Xuebao/Journal of Harbin Institute of Technology 47 (12), pp. 123-128, 2015
[21] Drosopoulos, G.A., Stavroulakis, G.E., Massalas, C.V. "Influence of the geometry and the abutments movement on the collapse of stone arch bridges", Construction and Building Materials 22 (3), pp. 200-210, 2008.
[22] Liu, B., Yang, C., Zhou, K. "Document Effect of springing displacement on mechanical performance of the buried corrugated steel arch bridge", Wuhan Ligong Daxue Xuebao

(Jiaotong Kexue Yu Gongcheng Ban)/Journal of Wuhan University of Technology (Transportation Science and Engineering) 36 (3), pp. 441-444, 2012.
[23] Liu, S.-M., Wang, Z.-X., Zhu, C. "Method of temporarily carrying heavy vehicle on masonry arch bridge without strengthening", Beijing Gongye Daxue Xuebao/Journal of Beijing University of Technology 41 (10), pp. 1559-1565, 2015
[24] Yau, J.-D. "Vibration of parabolic tied-arch beams due to moving loads", Document International Journal of Structural Stability and Dynamics, 6 (2), pp. 193-214, 2006
[25] Yang, J.-X., Chen, W.-Z., Gu, R. "Analysis of dynamic characteristics of short hangers of arch bridge", Bridge Construction 44 (3), pp. 13-18, 2014
[26] Nikkhoo, A., Kananipour, H., "Document Numerical solution for dynamic analysis of semicircular curved beams acted upon by moving loads", Proceedings of the Institution of Mechanical Engineers, Part C: Journal of Mechanical Engineering Science 228 (13), pp. 2314-2322. 2014
[27] Türker, T., Bayraktar, A. "Structural safety assessment of bowstring type RC arch bridges using ambient vibration testing and finite element model calibration", Measurement: Journal of the International Measurement Confederation pp 33-45, 2014
[28] Calçada, R., Cunha, A., Delgado, R., "Dynamic analysis of metallic arch railway bridge", Journal of Bridge Engineering 7 (4), pp. 214-222, 2002
[29] Chen, S., Tang, Y., Huang, W.-J., "Visual vibration simulation of framed arch bridge under multi-vehicle condition", Gongcheng Lixue/Engineering Mechanics 22 (1), pp. 218-222, 2005
[30] Wallin, J., Leander, J., Karoumi, R. "Strengthening of a steel railway bridge and its impact on the dynamic response to passing trains", Engineering Structures 33 (2), pp. 635-646, 2011
[31] Michaltsos, G.T., "The influence of Centripetal and Coriolis forces on the dynamic response of light bridges under moving vehicles", J. of Dound and Vibration, 247(2), 261-277, 2001.
[32] Kounadis A.N. "An efficient and simple approximate technique for solving nonlinear initial and boundary-value problems", Comp. Mechanics, 9, 221-231, 1992.